A Ray-tracing Method to Analyzing Modulated Planar Fabry-Perot Antennas

Hougs, Mikkel Dahl; Kim, Oleksiy S.; Breinbjerg, Olav

Published in:
2015 Proceedings of 9th European Conference on Antennas and Propagation

Publication date:
2015

Document Version
Peer reviewed version

A Ray-tracing Method to Analyzing Modulated Planar Fabry-Perot Antennas

Mikkel Dahl Hougs, Oleksiy S. Kim, Olav Breinbjerg
Department of Electrical Engineering, Technical University of Denmark, DTU, Kgs. Lyngby, Denmark
mdho@elektro.dtu.dk

***Abstract*—A new approach for fast modelling of Fabry-Perot antennas with modulated partially reflective surfaces (PRS) using ray-tracing is proposed.**

For validation of the method, a configuration is introduced which consists of a cavity with a modulated PRS, fed internally by a magnetic dipole. The PRS consists of 18×18 square patches of varying size placed in a regular grid with a lattice constant of approximately $\lambda_0/3$ at $20\,\mathrm{GHz}$. The radiation pattern of the configuration is determined both by the presented model and by a full-wave solver which is used as a reference. The Directivity predicted by the model and the reference is $16.2\,\mathrm{dB}$ and $16.8\,\mathrm{dB}$ respectively which proves a good agreement.

I. Introduction

It has long been known that Fabry-Pérot (FP) antennas, consisting of a simple feed antenna located in a resonant cavity formed by a ground plane and a partially reflective surface (PRS), can exhibit high directivity [1]. One main advantage of such antennas is the simplicity of the feeding mechanism, when compared to other directive antenna such as arrays, requiring a complicated feed network, or reflectors and reflect-arrays, where the feed antenna needs to be placed in front of the reflecting surface.

The radiation mechanism can be explained in terms of a cylindrical leaky-wave mode with a complex radial propagation constant, $k_\rho = \beta - j\alpha$ (assuming $e^{j\omega t}$ time dependence) where $\beta \leq k_0$ and k_0 is the wave-number of free space [2].

The phase and amplitude distribution of the aperture field is related to the phase and leakage constant, β and α, respectively, and determines the radiation pattern.

Typically, FP antennas are designed by performing a dispersion analysis for a given uniform PRS to identify leaky modes. This can be done by using a transverse equivalent network (TEN) [3] where the cavity is modelled as a semi-infinite transmission line, truncated in a short circuit, representing ground, and with a shunt reactance, representing the PRS. The reactance is determined by modelling a unit cell of the PRS assuming an infinite periodic structure. For simple structures, such as patch arrays and wire-grids, approximate analytic expressions for the reactance exist [4]. The TEN model allows for easy determination of the radial propagation constant. It is however limited to uniform PRSs whose parameters do not vary with position.

Because the leaky waves are cylindrical and exponentially decaying, the radiation pattern will be limited to a conical or pencil beam; furthermore since the aperture field is inherently non-uniform, it is difficult to achieve a high aperture efficiency.

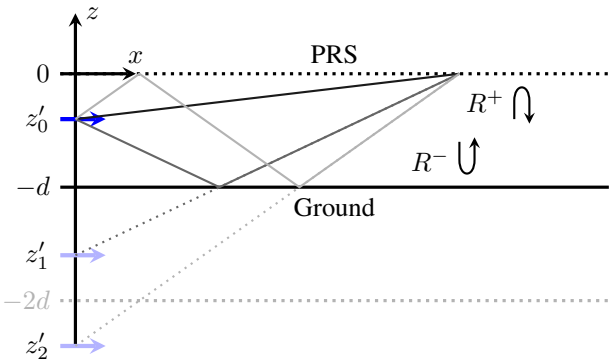

Fig. 1: An x-directed magnetic dipole located in a slab defined by complex plane wave reflection coefficients, R^+, R^-, and the transmission coefficient T^+.

In order to overcome these limitations, it may be advantageous to use a radially modulated PRS. Since the TEN model cannot be directly applied, an alternative model, based on the image theory and geometrical optics, is proposed and validated. The model is fast compared to full-wave solvers, making it suitable for optimization.

II. The Ray-tracing Method

The method takes outset in the radiation problem for an x-directed magnetic Hertzian dipole inside an infinite grounded slab. The slab is defined by its height d and plane wave reflection and transmission coefficients of the upper interface, R^+, T^+, respectively which generally depend on polarization and angle of incidence. The source is located at $\rho = 0$ and $z = z_0'$ as shown in Fig. 1.

The electric field of the dipole in a homogeneous medium can be expressed as a spectrum of plane waves which are transverse electric or magnetic with respect to their plane of incidence respectively. The boundary conditions are enforced by matching each plane wave using the reflection and transmission coefficients at the upper interface and the reflection coefficient of the ground plane which is -1 and 1 for the electric and magnetic field, respectively. The total field above the PRS is expressed in terms of Sommerfeld integrals [5]. The lower interface is chosen to be a ground plane for the sake of simplicity, but the method works for arbitrary surfaces which can be expressed in terms of plane wave reflection and transmission coefficients.

Generally, the reflection and transmission coefficients vary with angle of incidence, making it impossible to obtain analytical expressions for the Sommerfeld integrals. However, if it is assumed that they do not, and that the medium inside and above the slab is the same, the expression for the aperture field above the slab can be expressed as an infinite sum using the method described in [6]

$$\begin{aligned}\boldsymbol{E}_A(\rho,\phi,0^+) = \sum_{n=0}^{\infty} & T_n^{TE_z}\boldsymbol{E}_n^{TE_z}(\rho,\phi,z) \\ & + T_n^{TM_z}\boldsymbol{E}_n^{TM_z}(\rho,\phi,z)\end{aligned} \tag{1}$$

where $\boldsymbol{E}_n^{TE_z/TM_z}(\rho,\phi,z)$ is the field from an image source located at $z = z'_n$ radiating in a homogeneous medium as seen in Fig. 1. The expression for the magnetic field is obtained by replacing E with H in (1). The terms in the sum are added in chunks of 50 terms and if the relative change in magnitude is less than 10^{-6} after adding a chunk, the sum is truncated. The image points are obtained by repeatedly mirroring the original configuration in the lower interface, which gives

$$z'_n = \begin{cases} z'_0 - nd & \text{for even } n \\ -d - z'_0 - nd & \text{for odd } n \end{cases}. \tag{2}$$

Each coefficient $T_n^{TE_z/TM_z}$ is a product of the reflection coefficients which are encountered by a ray along its way from the source to an observation point, and the transmission coefficient of the upper layer at that point. This can be expressed as

$$T_n = s^n T(\rho) \prod_{i=1}^{\text{floor}(n/2)} R^+(\rho^+_{n,i}) \tag{3}$$

where for the TE case, $s = -1$ and R^+ and T are the reflection coefficients for the E-field, whereas for the TM case, $s = 1$ and R^+ and T are the reflection and transmission coefficients for the H-field. $\rho^+_{n,i}$ is a coordinate in the upper interface which can be written

$$\rho^+_{n,i} = \frac{z'_n - id}{z'_n}\rho. \tag{4}$$

The analytical expression for the decomposition of the incident field for an x-directed magnetic dipole can, for example, be obtained from the result presented in [7]. The decomposition allows for treatment of anisotropic PRSs which have distinct TE and TM reflection and transmission coefficients.

For a uniform PRS, the expression for the electric field is exact since it is the analytical solution to the Sommerfeld integral under the assumption that the surface can be fully described in terms of TE and TM reflection and transmission coefficients. For a modulated PRS, whose parameters vary slowly with position, so that it can be characterized locally by plane-wave reflection and transmission coefficients, the method works as a good approximation.

In order to simulate a realistic antenna, a square aperture centered above the source is chosen, and at the edges, vertical PEC walls are embedded. The effect of the truncation is modelled by placing images sources in a grid around the actual square aperture. The reflection and transmission coefficients above the image sources are found by repeatedly mirroring the PRS structure in the aperture sides.

Once the aperture field is obtained, the far field pattern is calculated by integrating the equivalent electric and magnetic currents in free space over the aperture. The radiated power is determined by integrating Poynting's vector over the aperture, and thus, the directivity can be obtained.

III. Validation for Modulated FP-antenna

In order to validate the method, a full wave simulation has been conducted using HFSS [8]. A modulated PRS consisting of 18×18 square patches in a square grid is placed at a distance $d = 8.07\,\text{mm}$ above an ground plane. This height is determined using the formula

$$\pi + \angle R_0 - \frac{4\pi}{\lambda_0}d = 0 \tag{5}$$

where R_0 is the reflection coefficient at $\rho = 0$ used in the ray-tracing method. Vertical PEC walls are placed at the edges of the PRS as described previously. In order to reduce the computation time, a PEC and PMC symmetry plane in the yz- and xz-plane, respectively, are introduced so that only a quarter of the antenna needs to be modelled. The HFSS model is shown in Fig. 2. To model an x-directed Hertzian magnetic dipole embedded in the ground plane, a quarter of a loop of small radius compared to the wavelength ($0.04\lambda_0$) is placed in the yz-plane centered around the origin and excited by a voltage source. The frequency is set to $20\,\text{GHz}$ with a lattice constant of $P = 5\,\text{mm} \approx \lambda_0/3$ giving an aperture side length of $L_a = 90\,\text{mm}$. The side length of each patch, L, is varied linearly with the distance between its center and the aperture center so that $L(0) = 4.8\,\text{mm}$ and $L(L_a/2) = 4.0\,\text{mm}$. The CPU time and real time for the last adaptive pass of the solver is approximately $30.0\,\text{h}$ and $3.75\,\text{h}$ respectively using $156\,\text{Gb}$ of memory on a 3GHz Xeon CPU.

The plane wave reflection and transmission coefficients are obtained from the expression for the surface impedance of an infinite patch array at normal incidence from [4]. This gives a reflection magnitudes of 0.88 for $L = 4.8\,\text{mm}$ and 0.79 for $L = 4.0\,\text{mm}$. The linearly decreasing reflection coefficients as a function of ρ is selected in order to more evenly distribute the leaked power over the aperture under the assumption that this might lead to a more uniform aperture field and thus higher directivity. Since it is hard to reach convergence in the HFSS model when the gaps between the patches are too small, the upper limit of the reflection coefficient is selected due to this consideration.

In Fig. 3, the radiation pattern of the model is compared to HFSS in the three planes defined by $\phi = 0°$, $\phi = 45°$ and $\phi = 90°$. Clearly the main beams agree very well. For $\phi = 0°$ and $\phi = 45°$, the agreement is good up to around $\theta = 60°$ and for $\phi = 90°$, the agreement is good up to around $\theta = 25°$. The maximum directivity from HFSS and the ray-tracing method is $16.8\,\text{dBi}$ and $16.2\,\text{dBi}$ respectively. Away from broadside,

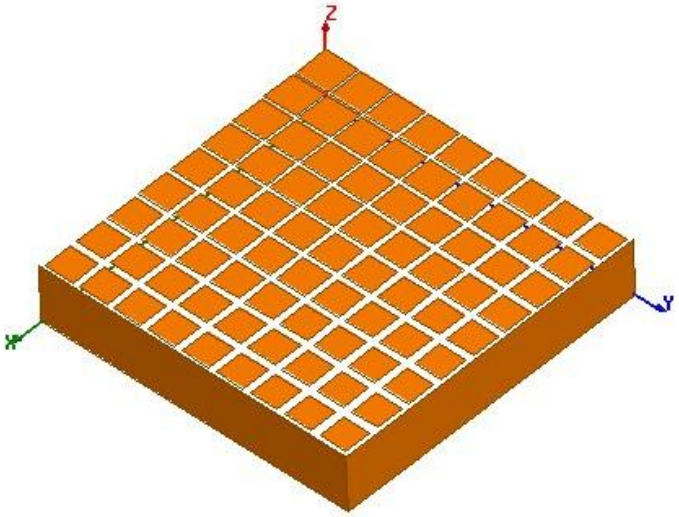

Fig. 2: HFSS model used for validation. The orange areas and the bottom of the cavity are PEC boundaries, the zx-plane is a PMC symmetry plane and the yz-plane is a PEC symmetry plane.

the discrepancy increases in both planes, but the side lobe level agrees well. This is caused by the inaccuracy of the assumptions made in the model: The description of the PRS in terms of reflection and transmission coefficients rely on the assumption of local periodicity and that the scattering can be expressed exclusively by the fundamental Floquet harmonic while in fact an infinite number of evanescent harmonics are present close to the surface. Furthermore, the truncation of the antenna is only handled approximately.

The CPU time of the current implementation is $572\,\mathrm{s}$ on a $3.2\,\mathrm{GHz}$ Xeon (6 cores and hyper-threading) processor using less than $60\,\mathrm{Mb}$ of RAM. Since the field in each point on the aperture can be computed independently, the program scales very well for multiprocessing and thus, the real time of the current simulation is $58\,\mathrm{s}$ including unnecessary overhead for plotting.

The fact that the main beam can be reproduced using this fast method proves that it can be valuable for optimizing and shaping the pattern of electrically large PRS antennas.

IV. Limitations of a single layer

It must be noted, that the modulation of the surface does in this case not increase the directivity when compared to a design with a uniform patch size of $4.8\,\mathrm{mm}$ (which is determined to $19.4\,\mathrm{dBi}$ using HFSS). This may be due to the fact, that a somewhat arbitrary variation of R is used and because the phase and magnitude of the reflection coefficient cannot be controlled independently.

The achievable values of the reflection and transmission coefficients of the PRS can be found using its TEN representation of a shunt reactance. This gives the following expressions for

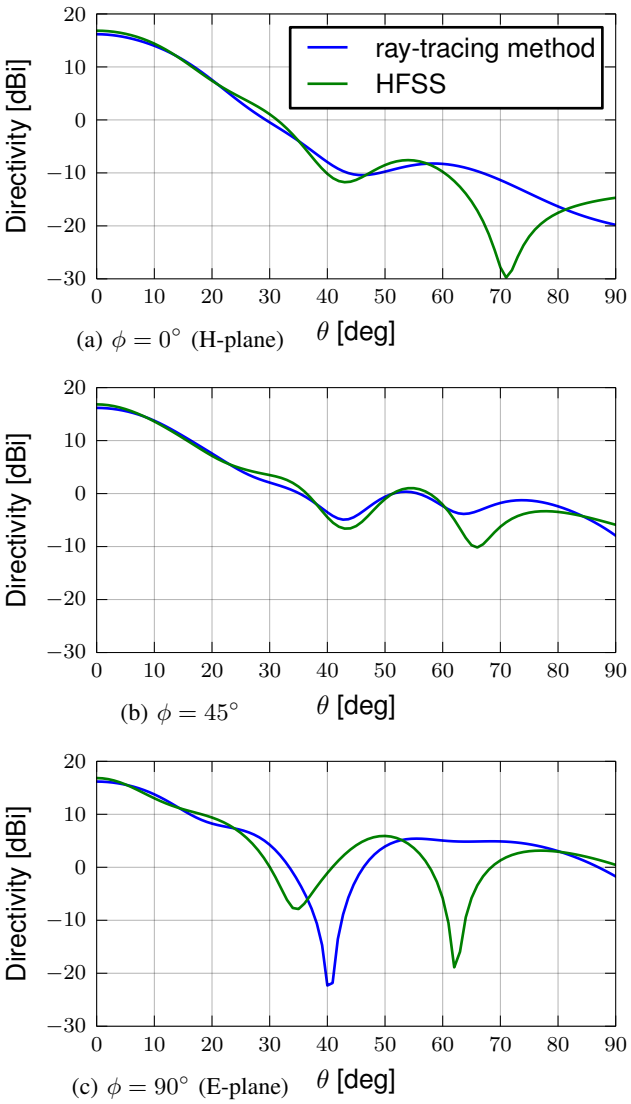

Fig. 3: Directivity patterns for E- and H-plane cuts calculated using the ray-tracing method versus the full wave HFSS simulation

the reflection and transmission coefficients of the E-field for a PRS in free space

$$R = \frac{-1}{j2\bar{X}+1} \tag{6}$$

$$T = R + 1 \tag{7}$$

where $\bar{X}$ is the reactance normalized to the free space intrinsic impedance. When $\bar{X}$ is varied from $-\infty$ to $+\infty$, the reflection coefficients will follow the path of a circle in the complex plane with center in $-1/2$ and radius $1/2$ as shown in Fig. 4. In the second and third quadrant, the reactance is inductive and capacitive respectively and in the limit where the reactance approaches 0 or $\pm\infty$ the PRS becomes a PEC or vanishes respectively. It is seen that around $R = -1$, the phase changes rapidly as a function of reflection magnitude, and thus,

modulating the reactance in order to obtain an aperture field with uniform magnitude will change the resonant behavior of the cavity which may be the reason why the directivity is not improved for the modulated PRS.

A way to overcome this limitation is to add a degree of freedom to the design by either using a modulated impedance surface instead of the ground plane or using a multi-layered PRS.

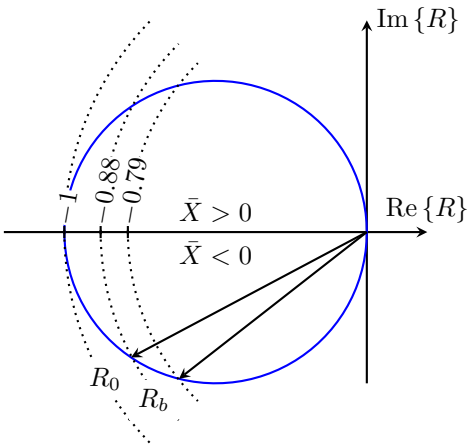

Fig. 4: Reflection coefficients of a single layered PRS plotted in the complex plane. The circle represent the achievable values and R_0 and R_b are the reflection coefficients of the upper and lower bound respectively of the modulated PRS used in Section III.

V. Conclusion

This paper presents a new ray-tracing method for calculating the directivity and radiation pattern of a FP antenna with a modulated PRS. The approach is valid for surfaces defined by TE and TM reflection and transmission coefficients which vary slowly with position. The goal of the research has been to show the validity of the method, which has been done by comparison with a full-wave solver. It has been shown that for the given test case, the patterns obtained by the ray-tracing method and HFSS are in good agreement up to $60°$ and $25°$ from broadside in the H-plane and E-plane respectively. Furthermore, a good agreement has been seen in the maximum directivities ($16.8\,\mathrm{dBi}$ and $16.2\,\mathrm{dBi}$ for HFSS and the model respectively) and the side lobe levels.

The main advantage of the method is its speed compared to a full wave solver. In the shown example, the ray-tracing method was used to produce a radiation pattern in less than a minute, whereas the HFSS-simulation took more than 3 hours. This makes the presented model useful for optimization

The next step is to produce a design with an optimized directivity. This may encourage the use of a multilayered PRS or a modulated impedance surface instead of a ground plane in order to obtain the degrees of freedom needed to appropriately tailor the phase and magnitude of the aperture field.

References

[1] G. Trentini, "Partially reflecting sheet arrays," *IRE Transactions on Antennas and Propagation*, vol. 4, no. 4, pp. 666–671, Oct. 1956.

[2] D. Jackson and A. Oliner, "A leaky-wave analysis of the high-gain printed antenna configuration," *IEEE Transactions on Antennas and Propagation*, vol. 36, no. 7, pp. 905–910, Jul. 1988.

[3] T. Zhao, D. R. Jackson, J. T. Williams, and A. A. Oliner, "General formulas for 2-D leaky-wave antennas," *IEEE Transactions on Antennas and Propagation*, vol. 53, no. 11, pp. 3525–3533, Nov. 2005.

[4] O. Luukkonen, C. Simovski, G. Granet, G. Goussetis, D. Lioubtchenko, A. V. Raisanen, and S. A. Tretyakov, "Simple and Accurate Analytical Model of Planar Grids and High-Impedance Surfaces Comprising Metal Strips or Patches," *IEEE Transactions on Antennas and Propagation*, vol. 56, no. 6, pp. 1624–1632, Jun. 2008.

[5] W. C. Chew, *Waves and fields in inhomogeneous media*. Van Nostrand Reinhold, 1990.

[6] A. Pirhadi and M. Hakkak, "An Analytical Investigation of the Radiation Characteristics Of Infinitesimal Dipole Antenna Embedded In Partially Reflective Surfaces to Obtain High Directivity," *Progress In Electromagnetics Research*, vol. 65, pp. 137–155, 2006.

[7] P. Clemmow, "The resolution of a dipole field into transverse electric and transverse magnetic waves," *Proceedings of the Institution of Electrical Engineers*, vol. 110, no. 1, p. 107, 1963.

[8] ANSYS HFSS, Version 15.0, ANSYS, Inc.